Structural and optical properties of $Zn_{0.9}Mn_{0.1}O$/ZnO core-shell nanowires designed by pulsed laser deposition

V. E. Kaydashev,[1,a)] E. M. Kaidashev,[1] M. Peres,[2] T. Monteiro,[2] M. R. Correia,[2] N. A. Sobolev,[2] L. C. Alves,[3] N. Franco,[3] and E. Alves[3]
[1]*Southern Federal University, 344090 Rostov-on-Don, Russia*
[2]*Departamento de Física and I3N, Universidade de Aveiro, 3810-193 Aveiro, Portugal*
[3]*Instituto Tecnológico e Nuclear, 2686-953 Sacavém, Portugal*

(Received 19 August 2009; accepted 1 September 2009; published online 3 November 2009)

Core-shell ZnO/ZnMnO nanowires on a-Al_2O_3 and GaN (buffer layer)/Si (111) substrates were fabricated by pulsed laser deposition using a Au catalyst. Two ZnO targets with a Mn content of 10% were sintered at 1150 and 550 °C in order to achieve the domination in them of paramagnetic MnO_2 and ferromagnetic Mn_2O_3 phases, respectively. Cluster mechanism of laser ablation as a source of possible incorporation of secondary phases to the wire shell is discussed. Raman spectroscopy under excitation by an Ar^+ laser revealed a broad peak related to the Mn-induced disorder and a redshift in the A_1-LO phonon. Resonant Raman measurements revealed an increase in the multiphonon scattering caused by disorder in ZnO upon doping by Mn. Besides the UV emission, a vibronic green emission band assisted by a ~71 meV LO phonon is also observed in the photoluminescence spectra. Core-shell structures with smooth shells show a high exciton to green band intensity ratio (~10) even at room temperature. © *2009 American Institute of Physics*. [doi:10.1063/1.3253572]

I. INTRODUCTION

Core-shell nanowires (NWs) have recently attracted considerable attention as possible candidates for building blocks of nanoscale devices in photonics, spintronics, and magneto-optics. Being a wide band gap semiconductor with a large exciton binding energy (60 meV), ZnO is an ideal host material for UV applications.

A prediction that ZnO doped with Mn would show above room temperature ferromagnetism made by Dietl *et al.*[1] have stimulated poignant interest in the field of experimental research of ZnO-based materials as promising candidates for diluted magnetic semiconductors. Whereas the absence of above room temperature ferromagnetism in ZnO doped by such transition metals as Mn and Co is reported by many authors,[2,3] the nature of possible defect-related high-temperature ferromagnetism is not absolutely clear.[4] Considerable research efforts have been focused on the synthesis and characterization of ZnO-based materials in the form of films, NWs, and core-shell structures.[5–7] The idea of designing new functional devices for photonics and spintronics on the base of these nanostructured materials, integrating both optical and magnetic properties, is especially topical.

In the present paper we report the fabrication of ZnO/ZnMnO core-shell nanostructures on a-Al_2O_3 and GaN (buffer layer)/Si (111) substrates and the investigation of their optical and structural properties.

II. EXPERIMENT

ZnO nanowires were grown by pulsed laser deposition (PLD) in argon flow [50 SCCM (SCCM denotes cubic centimeter per minute at STP)] at high pressure (100 mbar) using Au catalyst-assisted vapor-solid-liquid mechanism as described elsewhere.[8] The temperature of the substrate was maintained at 830 °C. The shell, a $Zn_{0.9}Mn_{0.1}O$ film (1000–2500 laser pulses), was deposited by the off-axis PLD method at an oxygen pressure of 0.2 mbar and a substrate temperature of 550 °C. Two targets with Mn content of 10% were prepared by mixing and pressing appropriate amounts of ZnO and MnO_2 powders. Both targets were sintered for 12 h in air at 1150 and 550 °C, respectively. Two different temperatures of target synthesis were chosen for the preparation of targets with the domination of the paramagnetic MnO_2 (1150 °C) and ferromagnetic Mn_2O_3 (550 °C) phases. The cluster mechanism of target ablation discussed in Ref. 9 for Mn-doped ZnO films should lead to a change in the magnetic behavior of the samples. Targets sintered at 1150 and 550 °C yielded a consistent and a friable compound, respectively.

The surface morphology of the grown structures was analyzed by scanning electron microscopy (SEM) as shown in Fig. 1. As observed, the morphology changes from snow-like to smooth when using targets sintered at 550 and 1150 °C, respectively. The diameter of the core-shell structures is seen to vary from 150 to 300 nm in the first case and from 50 to 100 nm in the second.

RT Raman spectra were recorded in a backscattering geometry using a Jobin Yvon T64000 and a Horiba Jobin Yvon HR 800 UV Raman spectrometers. The 488 nm line from a cw Ar^+ ion laser and the 325 nm line from a HeCd laser were used as excitation sources, respectively. The diameter of the analyzed spot was about 1 μm, and the spectra were taken with a wave number accuracy of 1 cm^{-1}.

Photoluminescence (PL) measurements were carried out with the 325 nm He–Cd laser line using a power density less

a)Electronic mail: kaidashev_mst@mail.ru.

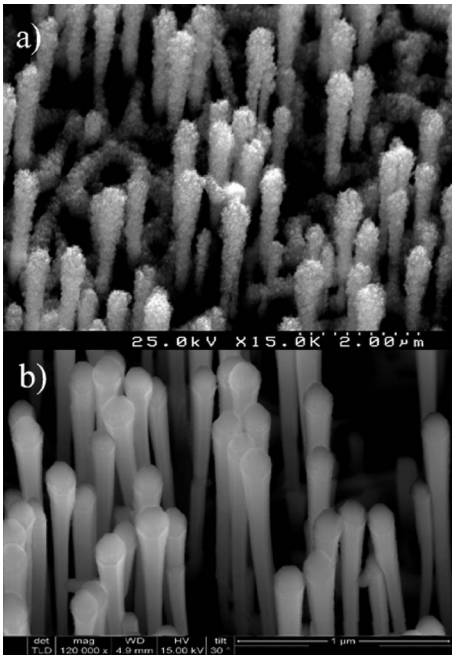

FIG. 1. SEM images of $Zn_{0.9}Mn_{0.1}O/ZnO/a\text{-}Al_2O_3$ core-shell nanowires. The $Zn_{0.9}Mn_{0.1}O$ shells were grown from targets sintered at (a) 550 and (b) 1150 °C, respectively.

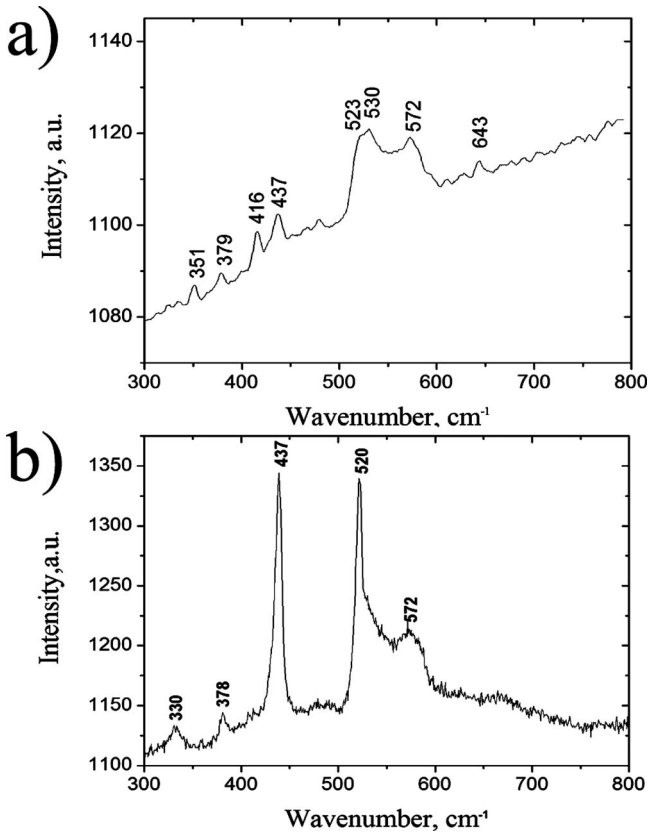

FIG. 2. Raman spectra of (a) $Zn_{0.9}Mn_{0.1}O/ZnO/Al_2O_3$ and (b) $Zn_{0.9}Mn_{0.1}O/ZnO/GaN$ (buffer layer)/Si (111) core-shell nanowires under Ar^+ ion laser (488 nm) excitation.

than 0.6 W/cm^2. The PL was measured between 5.8 and 300 K, and the samples were excited under an angle of 15° to the surface normal with the PL emission being collected along the surface normal. The emission was dispersed by a Spex 1704 monochromator (1 m, 1200 mm^{-1}) and detected by a cooled Hamamatsu R928 photomultiplier.

III. RESULTS AND DISCUSSION

The wurtzite structure of ZnO has the space group C^4_{6v} with two formula units per primitive cell with all atoms occupying C_{3v} sites. Each Zn atom is tetrahedrally coordinated to four O atoms and vice versa. At the Γ-point of the Brillouin zone the optical phonons of wurtzite ZnO have the irreducible representation $\Gamma=A_1+2B_1+E_1+2E_2$,[10] as predicted by the group theory.

The B_1 modes are silent in the Raman scattering and A_1 and E_1 are polar vibration modes splitting up into transverse optical (TO) and longitudinal optical (LO) phonons, due to the macroscopic electric field associated to LO phonons. The nonpolar E_2 modes are Raman active and have two frequencies, namely, E_2(high) and E_2(low) associated with the motion of oxygen atoms and zinc sublattice, respectively.[11] For highly *c*-oriented ZnO crystals, if the light is exactly normal to the surface, only the A_1(LO) and E_2 modes are observed, and the other modes are forbidden according to the Raman selection rules.

Figure 2 shows the RT Raman spectra of the studied samples under Ar^+ ion laser (488 nm) excitation. Phonon scattering was observed at 351, 379, 416, 437, 523, 530, 572, and 643 cm^{-1}. The peak at 437 cm^{-1} is commonly attributed to the E_2(high) nonpolar mode.[10–12] Two broad shoulders were observed in the range from 515 to 580 cm^{-1}. A line at 572 cm^{-1} ascribed to A_1(LO) (Refs. 10–12) is redshifted by about 2 cm^{-1}, which correlates with the results reported in Ref. 13. We consider that this redshift is due to strain effects and disorder induced by the Mn doping of the shell. Schumm *et al.*[13] associated this shift with oxygen deficiency. The broad peak of Mn-induced disorder[12,13] has weak peaklike features at 517–523 and 528–530 cm^{-1}, whose positions depend on the localization of the excitation spot on the sample surface. The peaks observed at 416 and 643 cm^{-1} are associated to the Raman active vibrational modes of the $a\text{-}Al_2O_3$ substrate. The line at 351 cm^{-1} is due to the plasma emission from the laser tube. The appearance in the Raman spectra of the A_1(TO) ZnO phonon at 379 cm^{-1} (Refs. 11 and 12) reveals that nanowires are tilted with respect to the surface normal.

The Raman spectra of $Zn_{0.9}Mn_{0.1}O/ZnO/GaN$ (buffer layer)/Si (111) contained the E_2(high) nonpolar mode (437 cm^{-1}) of ZnO as well as a peak related to the Mn-induced disorder at about 525 cm^{-1}, which overlaps with the stronger Si peak at 520 cm^{-1} and A_1(LO) at 572 cm^{-1}, redshifted by about 2 cm^{-1}. Besides, two lines at 330 and 378 cm^{-1} were observed. Calleja and Cardona[14] attributed a close peak at 332 cm^{-1} to the second-order band of ZnO.

Figure 3 shows the RT Raman spectra of a $Zn_{0.93}Mn_{0.07}O/Al_2O_3$ film under excitation by 325 nm. The film was deposited at the same conditions as the NW using a target with Mn content of 7% sintered at 550 °C.

Resonant Raman spectra revealed only the A_1(LO) phonon scattering and its overtones analogous to the spectra ob-

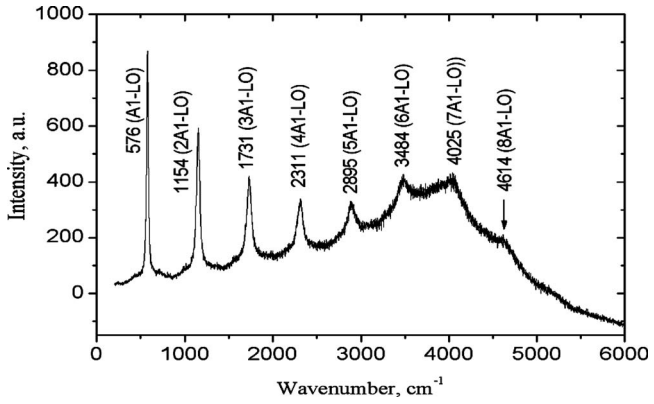

FIG. 3. Resonant Raman spectra of the $Zn_{0.93}Mn_{0.07}O/Al_2O_3$ film measured at 300 K.

served in Ref. 15 for ZnO doped by such transition metals as Mn, Co, Cu, and Ni. Phonon overtone scattering in ZnO is relevant for the A_1(LO) and E_1(LO) phonons. Multiple overtones of the E_1(LO) phonon in bulk ZnO were investigated in Refs. 14 and 16. In the case of the ZnO film on the a-Al_2O_3 substrate in the excitation geometry parallel to the c-axis of ZnO, scattering by the E_1(LO) phonon is forbidden according to the selection rules, and the corresponding Raman peak is not observed. Mn-induced disorder in the ZnO structure relaxes the Raman selections rules. As a result, phonons outside of the Brillouin zone center are activated leading to multiple overtone scattering.

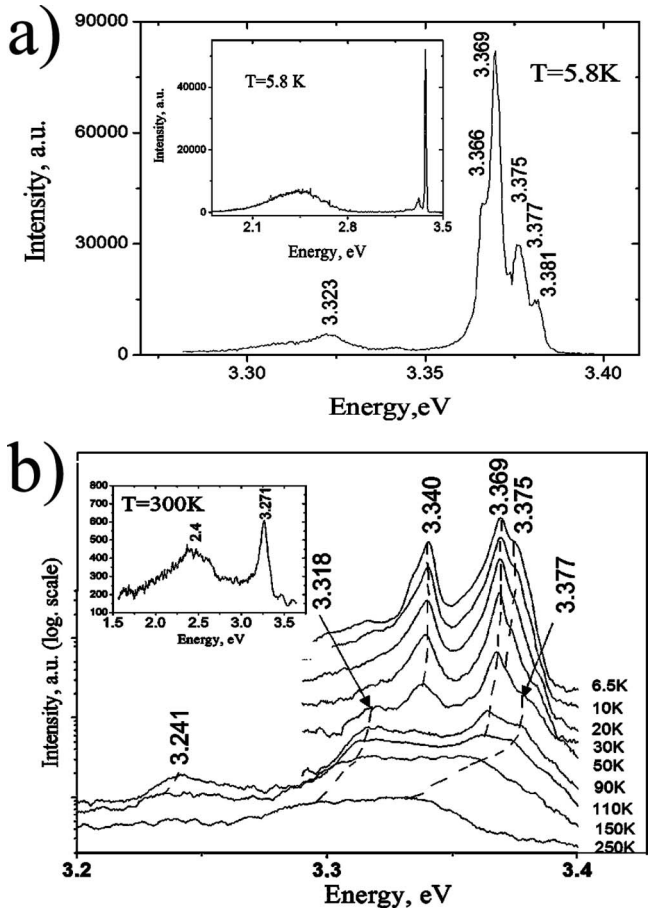

FIG. 4. PL spectra of $Zn_{0.9}Mn_{0.1}O/ZnO/a$-Al_2O_3 core-shell structures with (a) snowlike shells and (b) smooth shells.

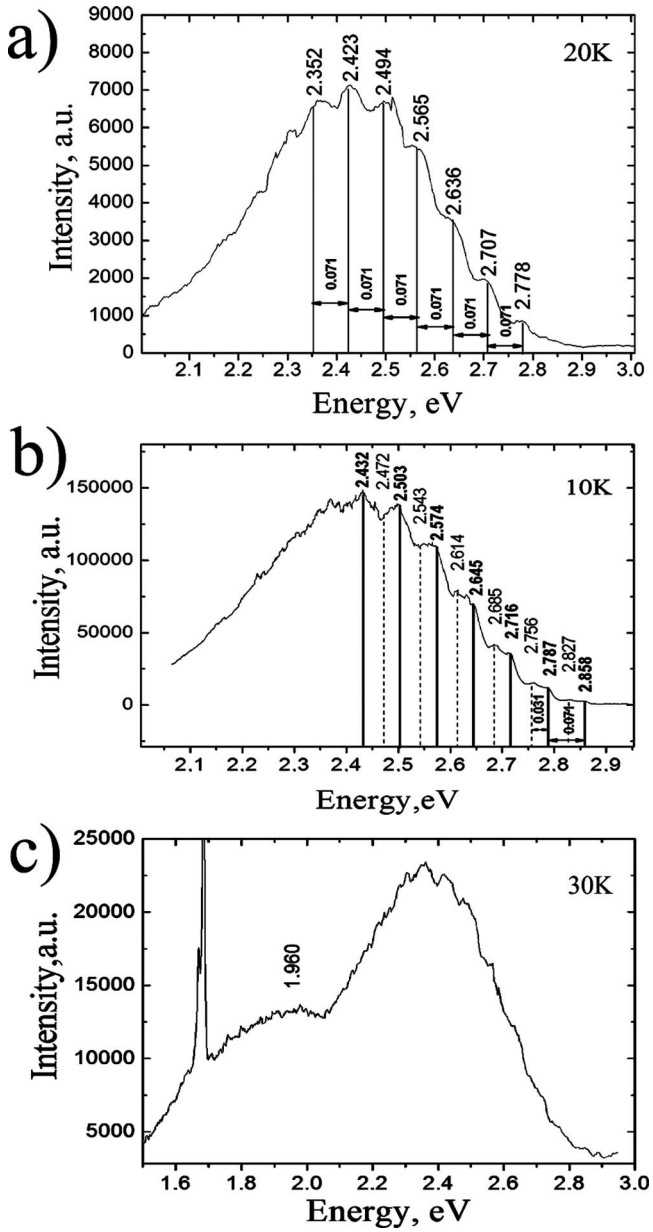

FIG. 5. PL spectra in the green/red spectral region of the $Zn_{0.9}Mn_{0.1}O/ZnO$ core-shell structures (with snowlike shells) grown on (a) an a-Al_2O_3 and (b) on a GaN (buffer layer)/Si (111) substrate, as well as of (c) a sample with smooth shells. The spectra were taken at different temperatures indicated in the respective panels.

The high-energy PL spectra observed at a low temperature are shown in Fig. 3(a). For the $Zn_{0.9}Mn_{0.1}O/ZnO$ core-snowlike-shell structures the emission spectra reveal the free exciton peaks $FX_A^{n=1}(\Gamma_5,\Gamma_6)$ at 3.377 and 3.375 eV.[17] In the near band edge spectral range, the most intense recombination occurs at 3.369 and 3.366 eV. The latter lines have commonly been associated to the recombination of donor bound excitons.[17,18] The peak at 3.381 eV has been assigned to the longitudinal exciton [upper polariton branch (UPB_A)].[17] However, also the $FX_A(n=2)$ and the FX_B have been reported at the same energy.[19] A weak and broad line at about 3.323 eV is located in the energy range expected for the two-electron recombination as previously proposed by Reynolds *et al.*[18] Figure 4(b) shows the temperature dependent

TABLE I. Sample composition as determined by PIXE (values in $\mu g/g$).

Mn	Error (%)	Zn	Error (%)	Ni	Error (%)	Cu	Error (%)
0.98	3	122	0.4	0.05	21	0.36	7

PL spectra of the $Zn_{0.9}Mn_{0.1}O/ZnO$ core-smooth-shell structure. The lines exhibit the usual excitonic behavior with characteristic temperatures analogous to those discussed in Ref. 20 with the high-energy RT PL being dominated by a recombination at 3.27 eV.

Besides the UV emission, deep level recombination is also observed in the measured PL spectra as can be seen in the inset of Fig. 4(a), in the spectrum taken at 5.8 K. Figures 5(a) and 5(b) show high-resolution spectra of the structured green emission for the $Zn_{0.9}Mn_{0.1}O/ZnO$ core-snowlike-shell samples grown on the a-Al_2O_3 and GaN (buffer layer)/Si (111) substrates, respectively. The emission band is vibronic assisted by a ~71 meV LO phonon, and our data are in accordance with those published by Dingle[21] who previously associated the emission to the presence of Cu^{2+} in the samples. Also, the two sets of fine structures equally separated by ~31 meV were identified in accordance with the data recently reported by Shi *et al.*[22] Particle induced x-ray emission (PIXE) analysis performed in the samples under study revealed that Cu is present in the nanorods (Table I).

The high optical quality of the produced samples can be claimed by the intensity ratio between the exciton-related and the green bands. Core-shell structures with smooth shells show a high I_{ex}/I_{green} ratio even at RT. The highest value at low temperature was found to be ~10. For this sample, an additional emission band in the orange/red spectral region is observed.

IV. CONCLUSIONS

Core-shell ZnO/ZnMnO nanowires on a-Al_2O_3 and GaN (buffer layer)/Si (111) substrates were fabricated by PLD using Au catalyst. The decrease in the PLD target synthesis temperature from 1150 to 550 °C leads to a change in the target compound from consistent to friable and to a change in the nanowire shell morphology from smooth to snowlike as a consequence. Doping of ZnO by Mn leads to a structural disorder which becomes apparent from the Mn-induced disorder shoulder and redshift in the A_1-LO phonon in the Raman spectra. Mn-induced disorder in the ZnO structure relaxes the Raman selections rules. As a result, phonons outside of the Brillouin zone center are activated leading to multiple overtone scattering under resonant excitation. Core-shell structures with smooth shells show a high exciton to green band intensity ratio (~10) even at room temperature.

ACKNOWLEDGMENTS

The work was supported by SANDiE Network of Excellence of the EU, by the FCT of Portugal (Project No. PTDC/FIS/72843/2006) and by Development of Higher School Science Potential, Russia (Project No. 2.1.1.6758/2009-2010).

[1] T. Dietl, H. Ohno, M. Matsukura, J. Cibert, and D. Ferrand, Science **287**, 1019 (2000).
[2] M. Snure, D. Kumar, and A. Tiwari, JOM **61**, 72 (2009).
[3] A. O. Ankiewicz, W. Gehlhoff, J. S. Martins, A. S. Pereira, S. Pereira, A. Hoffmann, E. M. Kaidashev, A. Rahm, M. Lorenz, M. Grundmann, M. C. Carmo, T. Trindade, and N. A. Sobolev, Phys. Status Solidi B **246**, 766 (2009).
[4] J. M. D. Coey and S. A. Chambers, MRS Bull. **33**, 1053 (2008).
[5] S. Han, D. Zhang, and C. Zhou, Appl. Phys. Lett. **88**, 133109 (2006).
[6] S. Han, C. Li, Z. Liu, B. Lei, D. Zhang, W. Jin, X. Liu, T. Tang, and C. Zhou, Nano Lett. **4**, 1241 (2004).
[7] B. Lei, S. Han, C. Li, D. Zhang, Z. Liu, and C. Zhou, Nanotechnology **18**, 044019 (2007).
[8] M. Lorenz, E. M. Kaidashev, A. Rahm, Th. Nobis, J. Lenzner, G. Wagner, D. Spemann, H. Hochmuth, and M. Grundmann, Appl. Phys. Lett. **86**, 143113 (2005).
[9] M. Diaconu, H. Schmidt, H. Hochmuth, M. Lorenz, G. Benndorf, D. Spemann, A. Setzer, P. Esquinazi, A. Poeppl, H. von Wenckstern, K. W. Nielsen, R. Gross, H. Schmid, W. Mader, G. Wagner, and M. Grundmann, J. Magn. Magn. Mater. **307**, 212 (2006).
[10] Ü. Özgür, Ya. I. Alivov, C. Liu, A. Teke, M. A. Reshchikov, S. Doğan, V. Avrutin, S.-J. Cho, and H. Morkoç, J. Appl. Phys. **98**, 041301 (2005).
[11] T. C. Damen, S. P. S. Porto, and B. Tell, Phys. Rev. **142**, 570 (1966).
[12] S. Venkataraj, N. Ohashi, I. Sakaguchi, Y. Adachi, T. Ohgaki, H. Ryoken, and H. Haneda, J. Appl. Phys. **102**, 014905 (2007).
[13] M. Schumm, M. Koerdel, S. Müller, H. Zutz, C. Ronning, J. Stehr, D. M. Hofmann, and J. Geurts, New J. Phys. **10**, 043004 (2008).
[14] J. M. Calleja and M. Cardona, Phys. Rev. B **16**, 3753 (1977).
[15] T. L. Phan, R. Vincent, D. Cherns, N. X. Nghia, V.V. Ursaki, Nanotechnology **19**, 475702 (2008).
[16] J. F. Scott, Phys. Rev. B **2**, 1209 (1970).
[17] A. Teke, Ü. Özgür, S. Dogan, X. Gu, H. Morkoç, B. Nemeth, J. Nause, and H. O. Everitt, Phys. Rev. B **70**, 195207 (2004).
[18] D. C. Reynolds, D. C. Look, B. Jogai, C. W. Litton, T. C. Collins, W. Harsch, and G. Cantwell, Phys. Rev. B **57**, 12151 (1998).
[19] M. Matlak, A. Molak, and M. Pietruszka, Phys. Status Solidi B **241**, R23 (2004).
[20] C. Boemare, T. Monteiro, M. J. Soares, J. G. Guilherme, and E. Alves, Physica B **308–310**, 985 (2001).
[21] R. Dingle, Phys. Rev. Lett. **23**, 579 (1969).
[22] S. L. Shi, G. Q. Li, S. J. Xu, Y. Zhao, and G. H. Chen, J. Phys. Chem. B **110**, 10475 (2006).